Long-lived stau, sneutrino dark matter and reconstruction of right-handed slepton masses

Avirup Ghosh

Harish-Chandra Research Institute

based on 10.1007/JHEP09(2018)143

in collaboration with Shankha Banerjee, Geneviève Bélanger and Biswarup Mukhopadhyaya

December 7, 2018

Motivations: Neutrino mass and Dark Matter

- Neutrino oscillation and Astrophysical data on DM(rotation curve, bullet cluster etc.) $\Rightarrow$ BSM theories
- SM gauge singlet right-handed neutrinos (ν_R) + Weekly Interacting Massive Particles (WIMP)($g_{WIMP} \sim 0.1$ and $m_{DM} \sim 100\,\mathrm{GeV}$)
- Null results from Direct-detection experiments + No evident of WIMP DM in MET($\not{E}_T$)+X channels in LHC.
- FIMP DM with negligible interaction strength with SM particles have been envisaged as an alternative possibility.
- Negligible interaction prevents FIMP DM to stay in equilibrium with thermal plasma and to be produced inside colliders
- Relic density is created from the decay of heavier bath particles $\Rightarrow$ Correct Relic demands FIMP interaction strength $\lesssim 10^{-10}$.

Neutrino mass and FIMP realization in $\tilde{\nu}$ MSSM

- R-parity conserved MSSM $\Rightarrow$ Naturalness, $\tilde{\chi}_1^0$ WIMP DM
- Neutrino oscillation data $\Rightarrow$ 3 generations of $\hat{\nu}_R$.
- With only Dirac type masses for νs $\Rightarrow$ $W_{\tilde{\nu}\text{MSSM}} = W_{\text{MSSM}} + y_\nu \hat{H}_u \hat{L} \hat{\nu}_R^c$.
- Neutrino oscillation data and cosmological bounds on neutrino masses $\Rightarrow 2.8\times 10^{-13} \lesssim y_\nu \lesssim 4.4\times 10^{-13}$.
- Such small couplings forces $\tilde{\nu}$ to stay out of equilibrium during the evolution of universe.
- FIMP $\tilde{\nu}$s are produced from the decay of other heavier superparticles (still in thermal equillibrium) and also from out-of-equilibrium decay of NLSPs, $\tilde{\tau}_1$ in our case $\Rightarrow \Omega_{\tilde{\nu}} h^2 = \frac{1.09\times 10^{27}}{g^{*\,3/2}} m_{\tilde{\nu}} \sum_i \frac{g_i \Gamma_i}{m_i^2} + \frac{m_{\tilde{\nu}}}{m_{\tilde{\tau}_1}} \Omega_{\tilde{\tau}_1} h^2$.

Collider signature of $\tilde{\nu}$ MSSM

- Small y_ν causes $\tilde{\tau}_1$ to be long-lived $\Rightarrow \Gamma_{\tilde{\tau}_1} \simeq \Gamma_{\tilde{\tau}_1 \to W \tilde{\nu}} = \frac{g^2 \tilde{\Theta}^2}{32\,\pi} |U_{L1}^{(\tilde{\tau}_1)}|^2 \frac{m_{\tilde{\tau}_1}^3}{m_W^2} \left[1 - \frac{2(m_{\tilde{\nu}}^2 + m_W^2)}{m_{\tilde{\tau}_1}^2} + \frac{(m_{\tilde{\nu}}^2 - m_W^2)^2}{m_{\tilde{\tau}_1}^4}\right]^{3/2}$, where $\tan 2\tilde{\Theta} = \frac{2\,y_\nu\, v\, \sin\beta\, |\mu \cot\beta - A_\nu|}{m_{\tilde{\nu}_L}^2 - m_{\tilde{\nu}}^2}$.
- For $m_{\tilde{\tau}_1} \sim 500\,\text{GeV}$, $m_{\tilde{\nu}} \sim 100\,\text{GeV}$ lifetime of $\tau_{\tilde{\tau}_1} \sim 1\,\text{sec}$ $\Rightarrow \tilde{\tau}_1$ behave as *heavy muons* inside the detector and decays only outside the detector.
- Large p_T-cut and cuts on the time delay between production and detection of $\tilde{\tau}_1$s in muon chamber (commonly known as β- cut) helps to distinguish $\tilde{\tau}_1$ from SM muons.
- The β distribution of the signal and background is shown:

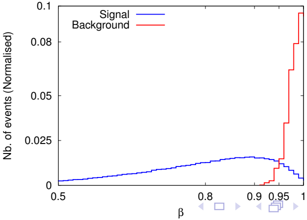

Collider signature of $\tilde{\nu}$ MSSM

- Given the $\tilde{\nu}$-LSP and $\tilde{\tau}_1$-NLSP specific mechanism of SUSY breaking dictates the N^{2}LSP, whether $\tilde{l}_R$ or $\tilde{\chi}_1^0$.
- Depending on the mass-orderings $m_{\tilde{\tau}_1} < m_{\tilde{l}_R} < m_{\tilde{\chi}_1^0}$ or $m_{\tilde{\tau}_1} < m_{\tilde{\chi}_1^0} < m_{\tilde{l}_R}$ we have two possible topologies,

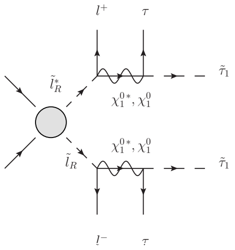

- Gives rise to two possible signals
  1. 2 $\tilde{\tau}_1$ + 2 same-flavour opposite sign leptons + 1 τ- tagged jet
  2. 2 $\tilde{\tau}_1$ + 2 same-flavour opposite sign leptons + 2 τ- tagged jets

Strategy of $M_{\tilde{l}_R}$ reconstruction

- **Signal 1:** Assymetric M_{T2} variable is used:
  $M_{T2} \equiv \min_{\vec{\not{p}}_{T1}+\vec{\not{p}}_{T2}=\vec{\not{p}}_T} \left(\max\left\{ m_T(\vec{p}_{T1}, \vec{\not{p}}_{T1}, m_1, m_{1\text{inv}}), m_T(\vec{p}_{T2}, \vec{\not{p}}_{T2}, m_2, m_{2\text{inv}}) \right\} \right).$

- **Signal 2:** Collinear approximation have been used to reconstruct the τs $\Rightarrow$ Assumption, $p^{\mu}_{\tau_{h_i}} = x_{\tau_{h_i}} p^{\mu}_{\tau_i}$ $\Rightarrow$
  $\vec{\not{p}}_T = (\frac{1}{x_{\tau_{h_1}}} - 1)\vec{p}_{\tau_{h_1}} + (\frac{1}{x_{\tau_{h_2}}} - 1)\vec{p}_{\tau_{h_2}}$, $\Rightarrow$ Solves to give $p^{\mu}_{\tau_{1,2}}$.

- SM backgrounds: $2\mu^{\pm} + 2\mu^{\pm}$ or $2e^{\pm} + 1$ or 2 τ-tagged jets $\Rightarrow$ ZZZ, ZZ, $t\,\bar{t}\,Z$, $Z\,h$ and $Z\,W^{+}\,W^{-}$.

- Basic cuts implemented for removal of SM backgrounds:

Parameter	$\tilde{\tau}_1$	$l^{\pm}$ GeV	j(jets)
p_T	> 70 GeV	> 10 GeV	> 20 GeV
$\beta(\mu$ only$)$	< 0.95	> 0.95	-
η	< 2.5	< 2.5	< 5

Table: Basic selection cuts applied to reduce SM backgrounds.

Strategy of $M_{\tilde{l}_R}$ reconstruction

- There are in principle identical final states originated by strongly interacting superparticles:

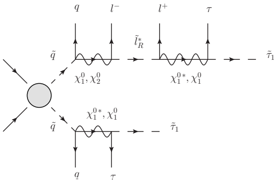

- Different topology $\Rightarrow$ decreases efficiency of our mass reconstruction techniques $\Rightarrow$Need to remove these events.

Parameter	$p_T(j_1)$	n(j) with $p_T(j) > 100$GeV	$\not{E}_T$
Cut Set A	<200 GeV	<2	<150 GeV
Cut Set B	<200 GeV	<2	<200 GeV

Table: Basic selection cuts applied to suppress the squark-gluino initiated processes.

- Isolation Cuts: $\Delta R(\tilde{\tau}_1, \tilde{\tau}_1) = \Delta R(\tilde{\tau}_1, j) = \Delta R(l, j) = \Delta R(j, j) \gtrsim 0.4$, and $\Delta R(l, l) \gtrsim 0.2$.

Results

- Some illustrative benchmarks are:

Masses(in GeV)	$m_{\tilde{\chi}_1^0} > m_{\tilde{l}_R}$	$m_{\tilde{\chi}_1^0} < m_{\tilde{l}_R}$
$m_{\tilde{\chi}_1^0}$	591	497
$m_{\tilde{l}_R}$	491	587
$m_{\tilde{\tau}_1}$	398	421

- Our results summarises as :

Cut Set	$N_s(\sqrt{S} = 14\mathrm{TeV}, \mathcal{L} = 3000\,\mathrm{fb}^{-1})$	
	$m_{\tilde{\chi}_1^0} > m_{\tilde{l}_R}$ Signal 1(Signal 2)	$m_{\tilde{\chi}_1^0} < m_{\tilde{l}_R}$ Signal 1(Signal 2)
Cut Set A	73(12)	45(11)
Cut Set B	79(13)	48(12)

Results

- **Signal 1:**
  The M_{T2}-distribution in each of the cases are shown below:

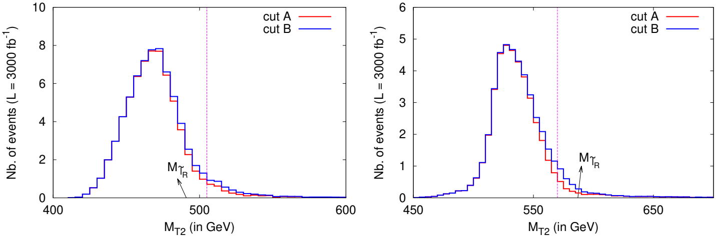

Results

- **Signal 2:**
  The invariant-mass distribution in each of the cases are shown below:

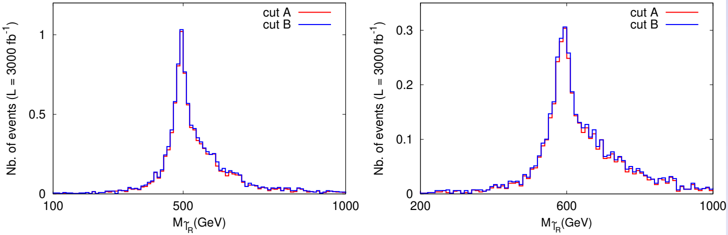

Conclusion

- Long-lived charged tracks, a very well-motivated signature of BSM physics have been discussed in the context of SUSY.
- Reconstruction of right-slepton masses with $5\% - 10\%$ accuracy have been carried out.
- Combined with earlier efforts of $\tilde{\tau}_1$-reconstruction [*JHEP*1607(2016)095] and $\tilde{\chi}_1^0$-reconstruction [*Phys.Rev.D*79(2009)115009] gives a good prescription for demysifying the nature of SUSY breaking.


Thank you
DesiComments.com

Back-ups

Freeze-In:

- Boltzmann eqn: If the production of a FIMP DM χ is via $A \to B\,\chi$,

$$Y_\chi \approx \frac{45}{(1.66)4\pi^4} \frac{g_A M_{Pl} \Gamma_A}{m_A^2\, g_*^{3/2}} \int_{x_{min}}^{x_{max}} dx\, x^3\, K_1(x) \qquad (1)$$

where $x = \frac{m_A}{T}$.
So, the total relic density,

$$\Omega_\chi h^2 \approx \frac{1.09 \times 10^{27}\, g_A}{g_*^{3/2}} \frac{m_\chi \Gamma_A}{m_A^2} \qquad (2)$$

$\Rightarrow$ see 10.1007/JHEP03(2010)080

- For the $\tilde{\nu}_R$-LSP possible decays are from $\tilde{\nu}_L\,,\tilde{l}_L\,,\tilde{\chi}_i^0\,,\tilde{\chi}_i^\pm \Rightarrow$ Decay- widths can be found in 10.1103/PhysRevD.73.051301.

Back-ups

Strategy:

- Other possible NLSPs include $\Rightarrow$ Neutralino($\tilde{\chi}_1^0$), Chargino($\tilde{\chi}_1^{\pm}$), left-handed Sneutrinos($\tilde{\nu}_L$) and Stop($\tilde{t}_R$) .
- M_{T2} construction strategy
  Two pairs:
  1. one $\tilde{\tau}_1$, it's nearest lepton (μ or e)
  2. another $\tilde{\tau}_1$ and it's nearest lepton (μ or e)

  The τ-jet is combined with that pair the $\tilde{\tau}_1$ of which is nearest to it in $\eta - \phi$-plane.
- Collinear approximation strategy:
  We construct invariant masses of all possible $\tilde{\tau}_1 \, \tau \, l$- pairs and the particular pair with minimum difference have been taken.

Back-ups

Benchmarks

- Benchmark points for studying $m_{\tilde{\chi}_1^0} > m_{\tilde{l}_R}$ scenario $\Rightarrow$

Masses(in GeV)	Benchmark 1	Benchmark 2	Benchmark 3
$m_{\tilde{\chi}_1^0}$	591	810	902
$m_{\tilde{l}_R}$	491	684	813
$m_{\tilde{\tau}_1}$	398	554	655

- Benchmark points for studying $m_{\tilde{\chi}_1^0} < m_{\tilde{l}_R}$ scenario $\Rightarrow$

Masses(in GeV)	Benchmark 1	Benchmark 2	Benchmark 3
$m_{\tilde{\chi}_1^0}$	497	693	946
$m_{\tilde{l}_R}$	587	757	1006
$m_{\tilde{\tau}_1}$	421	599	831

Back-ups

Results

- The number of events at $\mathcal{L} = 3000\, fb^{-1}$, for $2\tilde{\tau}_1 + 1$ τ-tagged jet $+$ 2 OSSF $+ \not{E}_T$ signal

Cut Set	Benchmark Point	N_s	
		$m_{\tilde{\chi}_1^0} > m_{\tilde{l}_R}$	$m_{\tilde{\chi}_1^0} < m_{\tilde{l}_R}$
Cut Set A	BP1	73	45
	BP2	26	11
	BP3	10	2
Cut Set B	BP1	79	48
	BP2	31	12
	BP3	12	2

Back-ups

Results

- The number of events at $\mathcal{L} = 3000\, fb^{-1}$, for $2\tilde{\tau}_1 + 2$ τ-tagged jet $+$ 2 OSSF $+ \not{E}_T$ signal

Cut Set	Benchmark Point	N_s	
		$m_{\tilde{\chi}_1^0} > m_{\tilde{l}_R}$	$m_{\tilde{\chi}_1^0} < m_{\tilde{l}_R}$
Cut Set A	BP1	12	11
	BP2	7	3
	BP3	2	1
Cut Set B	BP1	13	12
	BP2	9	3
	BP3	3	1